coatings

MDPI

Article

Studies on Preparation and Characterization of Aluminum Nitride-Coated Carbon Fibers and Thermal Conductivity of Epoxy Matrix Composites

Hyeon-Hye Kim [1,2], Youn-Sik Lee [2], Dong Chul Chung [1] and Byung-Joo Kim [1,*]

[1] Multi-Functional Carbon Materials Research Laboratory, Korea Institute of Carbon Convergence Technology, Jeonju 54853, Korea; gusgp5065@naver.com (H.-H.K.); sonagiii@kctech.re.kr (D.C.C.)

[2] Department of Chemical Engineering, Chonbuk National University, Jeonju 54896, Korea; yosklear@jbnu.ac.kr

* Correspondence: kimbj2015@gmail.com; Tel.: +82-63-219-3710

Received: 10 July 2017; Accepted: 7 August 2017; Published: 10 August 2017

Abstract: In this work; the effects of an aluminum nitride (AlN) ceramic coating on the thermal conductivity of carbon fiber-reinforced composites were studied. AlN were synthesized by a wet-thermal treatment (WTT) method in the presence of copper catalysts. The WTT method was carried out in a horizontal tube furnace at above 1500 °C under an ammonia (NH_3) gas atmosphere balanced by a nitrogen using aluminum chloride as a precursor. Copper catalysts pre-doped enhance the interfacial bonding of the AlN with the carbon fiber surfaces. They also help to introduce AlN bonds by interrupting aluminum oxide (Al_2O_3) formation in combination with oxygen. Scanning electron microscopy (SEM); Transmission electron microscopy (TEM); and X-ray diffraction (XRD) were used to analyze the carbon fiber surfaces and structures at each step (copper-coating step and AlN formation step). In conclusion; we have demonstrated a synthesis route for preparing an AlN coating on the carbon fiber surfaces in the presence of a metallic catalyst.

Keywords: aluminum nitride (AlN); carbon fibers; copper catalyst; composites; thermal conductivity

1. Introduction

Thermal management has always been a major concern in the design of high frequency and power electronic devices. In order to avoid the malfunction of electronic devices, composites materials used in these devices should have high thermal conductivity and electrical insulator properties. Normally, high thermal conductive performance has been obtained by adding fillers due to the thermal conductive chains or networks produced by the fillers [1–5]. In order to improve the thermal conductivity of composites, various inorganic ceramic fillers with high thermal conductivity have been introduced into insulation composites; notable example include silicon nitride (SiN) [6–8], silicon carbide (SiC) [9], boron nitride (BN) [10,11], alumina oxide (Al_2O_3) [12–14], and alumina nitride (AlN) [15–17]. Among the various ceramic fillers, aluminum nitride is an important ceramic material that has attracted considerable attention due to its excellent thermal conductivity (82–170 W/mK) and electrical resistance (>10^{14} Ω·cm @ R.T.), as well as its high density, wide band gap, low dielectric constant, and low thermal expansion coefficient close to that of silicon [18–28]. It has good chemical stability and high hardness and is used in various structure refractory composite applications. AlN also leads to an increase in critical thermal shock [29,30]. A common characteristic of various AlN composites is their utility as thermal conducting filler in electronic industries.

Commonly, a high Poisson's ratio is required for a material to be used as heat transfer filler for thermal conduction, such as fibers, whiskers, and nanowires. However, the synthesis of AlN nanostructures via methods such as molecular beam epitaxy is complicated and expensive. In this

light, an industrial and low cost method is needed. To address the aforementioned issues, we report a low-cost method for synthesizing AlN nanostructures doped on a carbon fiber having extremely high Poisson's ratio. Carbon fiber is a material consisting of good thermal conductivity that does not have restrictions in terms of length and has high Poisson's ratio [31,32]. Preparation of hybrid filler, based on the ceramic and carbon fiber, can be a novel method compared with conventional AlN synthetic methods.

Generally, AlN nanowires, nanobelts, nanolayers, whiskers, nanorods, nanotips, nanofluid [33–35] and nanotubes have been synthesized mainly by several methods: an arc discharging process [36], direct nitridation [37,38], chloride-assisted growth [39], carbothermal reduction [40], gas reduction [41], a sublimation process (recrystallization) [42], metal-organic chemical vapor deposition [43], and catalytic growth using aluminum and carbon complex, among others [23,44,45]. Among the methods for synthesizing AlN, direct nitridation of aluminum powder is attractive because of the low cost of the raw materials and the simple nitridation setup.

This method is not suitable as an AlN synthesis method for inducing high thermal conductivity when used as a filler of a composite material. This is because the shape of the precursor that can be used is limited to spherical or particulate forms due to the characteristics to be produced at a high temperature, and since the shape of the final product, AlN, is also in the form of spherical particles, it can be limited in forming a thermal conduction network in the composite system. Although AlN synthesized from aluminum powder shows low cost and high crystallinity, it has a limitation as a filler for high thermal conductive composites because of the limit of Poisson's ratio.

In our previous report [8], SiN-coated carbon fibers were successfully manufactured by simple wet-thermal method using silane coupling agent, resulting in a hybrid filler with high Poisson's ratio and thermal conductivity. Therefore, it was deemed possible to apply this method to the production of AlN-coated carbon fibers. In this paper, by a direct wet-thermal method (WTT) process, AlN nanostructures with a hexagonal crystalline structure were synthesized at above 1500 °C. The complete synthesis is achieved at temperatures up to 1500 °C under flowing nitrogen-based gases and results in agglomerated AlN due to the low melting point of $AlCl_3$ which is less than the temperature required for nitridation. In addition, compared with other methods, this method is simple and requires inexpensive precursors.

To date, AlN having one-dimensional, two-dimensional and three-dimensional structure can be synthesized through various chemical routes as described above. However, these methods generally require high temperatures, substrates, catalyst and long-term production cycles [46]. Therefore, we proposed a new synthesis route for the production of AlN that can be synthesized at relatively low temperatures in a short time. Short reaction times, simple treatments and low processing costs can be achieved through the WTT method. In this study, the preparation and thermal properties of AlN synthesized by WTT method were analyzed according to the synthesis temperature and the use of catalyst.

2. Experimental

2.1. Sample Preparation

All starting materials were used without further purification. The aluminum nitride (AlN) nanolayers were fabricated by a wet-thermal treatment method (WTT) with a nitrogen/ammonium mix atmosphere. Five weight percent of Reagent-grade aluminum chloride powder ($AlCl_3$, purity 97%, DaeJung Chemical & Metals Co, Ltd., Siheung, Korea) was dissolved in a mixture of ethanol and water (a weight ratio of 95:5).

Prior to use carbon fibers (chopped-type carbon fiber, T300, Toray Co., Tokyo, Japan), each fiber samples were treated by 1.0 mol of nitric acid at room temperature for 30 min to remove surface impurities and form surface active sites such as phenolic hydroxyl groups which can help metal loading on fiber surface by enhanced physical adhesion strength such as polar-polar interaction.

Subsequently, acid-treated carbon fibers were coated with copper using the electroless process as described below. A first, pre-treatments of carbon fibers were prepared by sensitization and activation treatments. Samples were sensitized by dispersing them in a hydrochloric acid solution containing tin chloride ($SnCl_2$). The samples were then rinsed with distilled water. After rinsing, the surfaces were activated by adding the samples in another hydrochloric acid containing palladium chloride ($PdCl_2$) followed by washing thoroughly by with distilled water. These steps are necessary for the subsequent reactions during electroless plating. Details of the conditions used for each solution are shown in Table 1. Copper coated-carbon fibers were then added into an $AlCl_3$ solution for 60 min, filtered, and dried in an oven at 80 °C for 120 min.

Table 1. Electroless plating process of copper on carbon fibers.

Step	Process	Chemical	Concentration	Temperature (°C)	Time (min)
1	Sensitizing	$SnCl_2$/HCl	10 g/L 10 mL/L	35	30
2	Rinse	H_2O	–	25	5
3	Activator	$PdCl_2$/HCl	0.4 g/L 3 mL/L	40	30
4	Rinse	H_2O	–	25	5
5	Pd reduction	NaOH	100 g/L	25	60
6	Rinse	H_2O	–		
7	Copper plating	$CuSO_4 \cdot 5H_2O$ $KNaC_4H_4O_6$ NaOH $PbNO_3$ 37% HCOH	18 mL/L 120 m/L 24 mL/L 1 mL/L 9 mL/L	52–58	180

The synthesis of AlN nanostructures was investigated by varying the heating temperature conditions and was carried out in an alumina boat set in the center of an alumina tube mounted in a horizontal furnace. The furnace was heated to 1500 °C with a rate of 4 °C/min under a nitrogen gas (N_2) flow of 200 cc/min and maintained at 1500 °C for 60 min under a 1000 ppm concentration ammonia gas atmosphere. Ammonia (NH_3) gas flow of 100 cc/min was introduced to the tube. Finally, the sample was cooled to room temperature under the nitrogen atmosphere. Various temperatures conditions were applied using the same method as explained above, and this should explain name of various treated sample in this work (Table 2).

Table 2. Sample Names Denoted According to Treatment Conditions.

Treatment Conditions	Sample Name
As-received carbon fiber (CF)	ARCF
5 wt % of $AlCl_3$ treated CF	AlClF
Copper (Cu) coated carbon fiber	CuF
Cu coated CF added into 5 wt % of $AlCl_3$ solution	AlCuF
Synthesis of Al_2O_3 coated CF from $AlCl_3$ treated CF at 1500 °C without Cu	T15AOF
Synthesis of AlN coated CF from $AlCl_3$ and Cu hybrid treated CF at 1500 °C	T15ANF
Synthesis of AlN coated CF from $AlCl_3$ and Cu hybrid treated CF at 1600 °C	T16ANF
Synthesis of AlN coated CF from $AlCl_3$ and Cu hybrid treated CF at 1700 °C	T17ANF
ARCF reinforced epoxy matrix composites	NOFP
Synthesized T15ANF reinforced epoxy matrix composites	T15ANP
Synthesized T17ANF reinforced epoxy matrix composites	T17ANP

2.2. Composites Preparation

For this study, a mixture of bisphenol-A-diglycidyl (YD-128, KUKDO Chem., Seoul, Korea) and 4,4′-diamino dipheyl methane (DDM, TCI, Seoul, Korea) was prepared with a 1:0.25 equivalent weight

ratio in order to use the matrix of composites. First, DDM was grind to powder shape to reduce the dissolution time and added into YD-128 resin, and then the mixture was heated in an oil bath at 120 °C for 30 min. Compounding samples were prepared using as-received carbon fiber (ARCF) and AlN coated carbon fiber as a thermally conductive filler, respectively. Finally, each sample was cured using hot-press vacuum-bag-molding at 150 °C for 30 min with 7.5 MPa. The size of final composites was cut with 25 mm × 25 mm × 1 mm.

The fiber fraction (weight ratio) of all composites was fixed at 0.5 when the resin (epoxy + DDM) weight ratio was 1.

2.3. Characterization

The morphology and element composition of the samples was characterized by using field emission scanning electron microscopy (FE-SEM, SUPRA 40VP, 0.5–30 KV, Carl Zeiss Co., Oberkochen, Germany) as well as an energy X-ray dispersive spectroscopy (EDS, SUPRA 40VP, 0.5–30 KV, Carl Zeiss Co., Oberkochen, Germany) with mapping images. The samples were coated with platinum to enhance the image resolution and to prevent electrostatic charging. Additionally, high-resolution transmission electron microscopy (HR-TEM, JEM-ARM-200F, JEOL Co., Tokyo, Japan) was used to take images of synthesized products and their crystallite structure. The sheets were dispersed in ethanol by sonication for 10 min and some pieces were collected on carbon-coated 200-mesh copper grids for TEM observation. HR-TEM was equipped with selected-area electron diffraction (SAED). The crystalline phase identification of the samples was carried out by X-ray diffraction (XRD, X'pert^3 Powder, PANalytical Co., Almelo, The Netherlands). The diffraction data were collected in the range of 30–80° with a scan speed of 2°/s using Cu-Kα radiation (wavelength = 1.54056 Å). The thermal conductivity of the AlN-coated carbon fiber-reinforced composite was determined at room temperature by solid thermal conductivity equipment with transient thermal type measurement (TPS 500 S, Hot Disk AB Co., Göteborg, Sweden). Two identical samples were subjected to a thermal conductivity test using a 5465 sensor (including nickel wire and the polyimide insulation layer), and the end result was an average of three values.

3. Results and Discussion

The FE-SEM images of the samples with different surfaces treatments are shown in Figure 1. Elemental mapping analysis by EDS images were performed to confirm the elemental changes of the fiber surface according to each aluminum chloride ($AlCl_3$) and copper (Cu) surface treatment. The image of acid-treated carbon fiber is shown in Figure 1a. The shapes of the fiber surfaces treated with $AlCl_3$ (AlClF), Cu plating (CuF) and hybrid coating (AlCuF) were compared and shown. The hybrid coating was coated by a simple method of immersing Cu-plated carbon fibers in an $AlCl_3$ solution. The prepared hybrid coating sample of Figure 1d showed a spotty-shape on the surfaces of the carbon fiber, and the EDS mapping results show that the Al (red) and Cu (yellow) source on the carbon fiber surfaces and is a mixed pseudocolor representation of both images (Figure 1e). Figure 1f shows a schematic representation of the formation of the AlCuF.

Figure 2 shows XRD and EDS analysis results of sample synthesized from $AlCl_3$ treated carbon fibers (AlClF) without the copper coating step, which was synthesized form AlClF under flowing N_2 and NH_3 at 1500 °C for 1 h. As presented in Figure 2b, the EDS image taken of the surface of the T15AOF can mean the Al_2O_3 phase due to the presence of Al and oxygen. This result is correlated well with the XRD results of Al_2O_3, which is T15AOF shown in Figure 2a. No characteristic peak associated with other crystalline forms was detected in the XRD results, indicating that the sample is predominantly Al_2O_3. In comparison, Figure 3 shows the XRD results of samples synthesized at various temperatures with copper coating, acting like metallic catalyst, from AlCF. As observed in Figure 2a, a corresponding crystalline peak of typical AlN was not founded in T15AOF. Meanwhile, T15ANF showed some crystalline peaks of AlN at almost same preparation conditions with T15AOF except the presence of copper layer on the fiber surface.

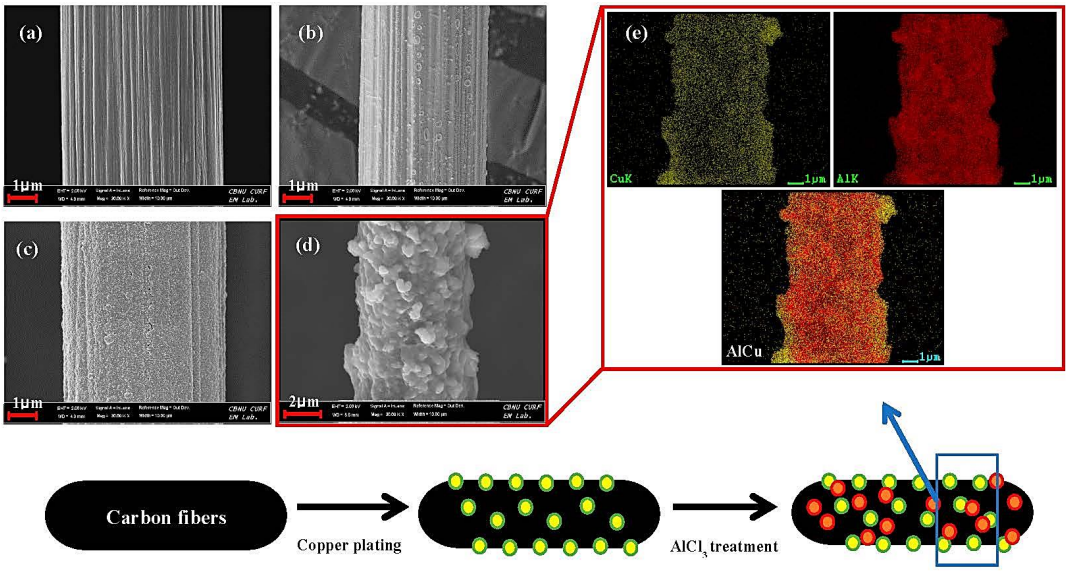

Figure 1. FE-SEM images of the as-synthesized sample with different surface treatments: (**a**) as-received carbon fiber (ARCF), (**b**) 5 wt % of $AlCl_3$ treated carbon fiber (AlClF), (**c**) copper coated carbon fiber (CuF) and (**d**) copper coated carbon fiber added into 5 wt % of $AlCl_3$ solution (AlCuF), (**e**) Energy dispersive X-ray spectroscopy (EDS) images of the (**d**) AlCuF. EDS image of the mixed pseudocolor representation Al and Cu complex treatment CF. Elemental mapping image of Cu and Al is shown in yellow and red, respectively. (**f**) Schematic representation of the formation AlCuF.

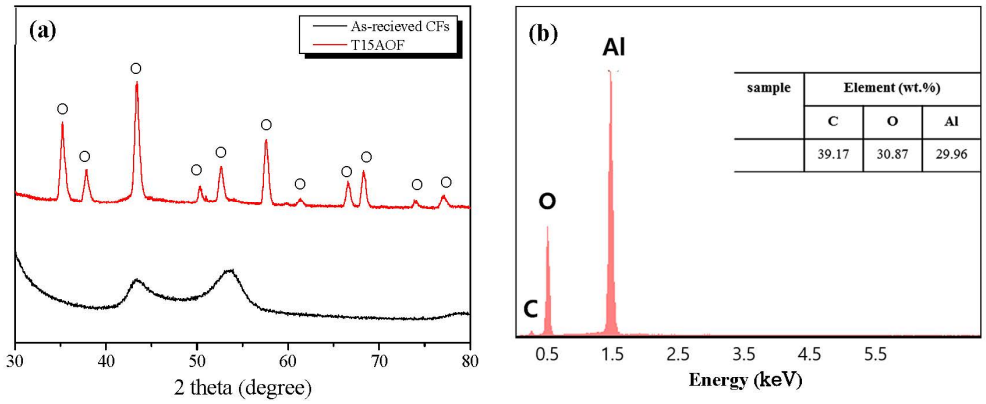

Figure 2. (**a**) XRD patterns of the products synthesized at 1500 °C for 1 h in 1000 ppm NH_3 atmosphere balanced by N_2 (T15AOF); (**b**) EDS spectrum of the middle of the (**a**) T15AOF.

It is well-known fact that the surface of carbon fibers has 10 to 15 percent of oxygen atoms [47]. When oxygen is present during AlN synthesis, Al-O bonds are formed more easily than Al-N bonds. For this reason, oxygen-free conditions are essential. Al-O is mainly formed by the oxygen released by the decomposition of the surface functional group of the carbon fiber during the high-temperature heat treatment, which is already confirmed in Figure 2. However, when the copper layer is present between the carbon fiber and the aluminum chloride, oxygen-free conditions can be formed because it acts as a trap to absorb oxygen molecules (formation of Cu_x-O_y) generated from the carbon fiber during the heat treatment. This condition can accelerate the formation of Al-N on carbon surfaces. On the other hand, it was confirmed that the crystallization of Al-N was increased and the Al-O was scarcely observed as the heat treatment temperature became closer to 1700 °C.

Furthermore, in order to investigate the effect of reaction temperature on the production of AlN nano-layers, the precursor from AlCuF was thermally treated at temperature of 1500 °C–1700 °C in

a nitrogen-based gas. The increased temperature stimulated the growth and aggregation of the AlN crystallites. Figure 3 shows that as the reaction temperature increases, the (100) peak of XRD and AlN products formation is completed. As the synthesis temperature increased, the 110 peak at 33.3° became narrower in shape and the intensity became stronger. The Al_2O_3 peak was decreased and the formation of AlN was increased in the product as the reaction temperature was increased. It was observed that the T15ANF was composed of two phases; hexagonal AlN and Al_2O_3, and Synthesis of AlN coated carbon fibers from $AlCl_3$ and copper hybrid treated carbon fibers at 1600 °C (T16ANF) was implying the transformation of Al_2O_3. A few weak peaks were also found in the XRD patterns, and they originate from the remaining Al_2O_3. However, the T17ANF only contained one phase; hexagonal AlN. XRD patterns of T17ANF prepared at high temperature did not exhibit any detectable peaks other than those assigned to AlN (Synthesis of AlN coated carbon fibers from $AlCl_3$ and copper hybrid treated carbon fibers at 1700 °C), as shown in Figure 3a. This demonstrated that as the temperature increased, the Al_2O_3 gradually disappeared and then pure AlN was obtained. The AlN phase of the three samples indexed as hexagonal AlN and the three intense peaks at 2θ = 33.3°, 38.1°, 59.5° were assigned to the plane of hexagonal AlN (100), (101), and (110), respectively, agreeing well with the calculated diffraction patterns. The overwhelming (002) peak implies that the AlN nanostructures grow preferentially along the *c*-axis. The corresponding structural model is presented in Figure 3. As shown in Figure 3, the growth of AlN crystals is caused by the combination of continuous Al and N atoms at the edge region [45,48].

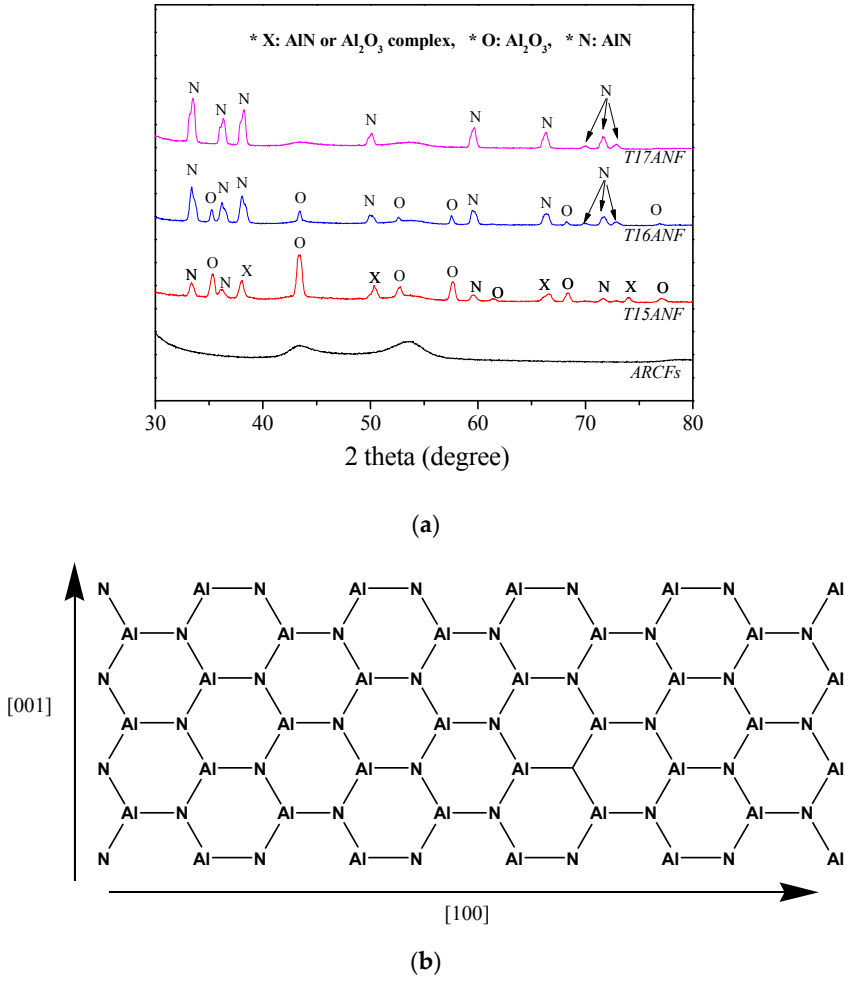

Figure 3. (**a**) XRD patterns of the products obtained from AlCuF as a function of reaction temperature for 1 h; (**b**) the schematic representation of the structural model of AlN formed at 1700 °C on the fiber.

Table 3 shows the results of analysis of the L_a and L_c values of the samples synthesized at different temperatures. In the case of T15ANF, it was confirmed that L_a and L_c values were the highest. On the other hand, in the case of T16ANF, L_a and L_c values were significantly reduced as compared with those of T15ANF, and T17ANF was slightly increased compared with T16ANF. The XRD results in Figure 3 show that T15ANF contains a high content of Al_2O_3. In T16ANF, AlN is a major component, and some Al_2O_3 was observed, and Al_2O_3 was not observed at all in T17ANF, indicating that it is a crystal structure composed of AlN.

Table 3. The crystallite height (L_c) and width (L_a) of AlN and the interlayer spacing values obtained from XRD.

Samples	002 Peak				100 Peak			
	2θ	d_{002} (Å)	FWHM	L_c (Å)	2θ	d_{100} (Å)	FWHM	L_a (Å)
T15ANF	36.21	2.480	0.4436	1043.83	33.38	2.683	0.4799	59.80
T16ANF	36.27	2.476	0.5737	807.32	33.44	2.679	0.5792	49.56
T17ANF	36.25	2.477	0.5550	834.41	33.43	2.680	0.5493	52.25

The reported lattice constants [49] of Al_2O_3 are L_a = 4.785 (Å) and L_c = 12.99 (Å). On the other hand, the lattice constant of AlN has L_a = 3.11 (Å) and L_c = 4.98 (Å), which are smaller than Al_2O_3. Based on the above report, it can be seen that T15ANF shows the highest L_a and L_c values because it has a mixed crystal phase of Al_2O_3 and AlN but Al_2O_3 rich composition.

In the case of T16ANF, it is considered that the Al_2O_3 peak is decreased and AlN peak is enhanced as the temperature is increased. It is thinkable that the value of L_c and L_a is remarkably decreased because Al_2O_3 having a relatively large crystal size is predominantly decreased. T17ANF has a slightly increased lattice constant value compared to T16ANF, which can be resulted by the influence of the crystal peaks of AlN grown perfectly as compared with the unstable AlN peak of T16ANF as the temperature increases.

Figure 4 shows the result of elemental analyzing the surface composition of the synthesized sample using EDS in more detail. EDS results show that the content of N element in T15ANF can be considered to be almost insignificant. T15ANF is composed of Al_2O_3 with a small amount of AlN, but it is considered that relatively weak N element was not detected as compared with Al and O elements. (N element is not detected maybe due to the limit of the instrumental resolution.) As the reaction temperature was increased to 1700 °C (T17ANF), while, the O element decreased and the N element increased. From the surface composition analysis of the samples via EDS, it was confirmed that the amount of N element increased as the reaction temperature was raised. Therefore, it could be concluded that the synthesis of AlN could be controlled by the use of the copper layer and adjusting the reaction temperature.

Figure 5 shows the TEM images of the synthesized T15ANF and T17ANF samples. The T15ANF samples were composed of bough (or twig)-shaped nanocrystallites. In the case of T15ANF showing crystal peaks in which Al_2O_3 and AlN are mixed (XRD in Figure 3), a TEM image of a typical twig shape can be identified by mixing Al_2O_3 in powder or particulate form [50] and AlN form showing plate or linear shape [51,52] (Figure 5a). T17ANF shows a typical AlN crystal peak, and the corresponding TEM image also shows a linear shape. The selected area electron diffraction (SAED) of the samples is inserted in Figure 5 and the crystal indices are calibrated in the photograph. According to the calibration of the diffraction lattice, it is determined to be hexagonal AlN (Figure 5b insert images), which is consistent with the results of the Figure 3b in XRD pattern. In the EDS analysis, the T17ANF showed that the chemical composition mainly consisted of Al and N element (Figure 4c). The SAED pattern of the AlN (Figure 5b) indicated a crystalline nature with a [110] zone axis and the growth direction along [001].

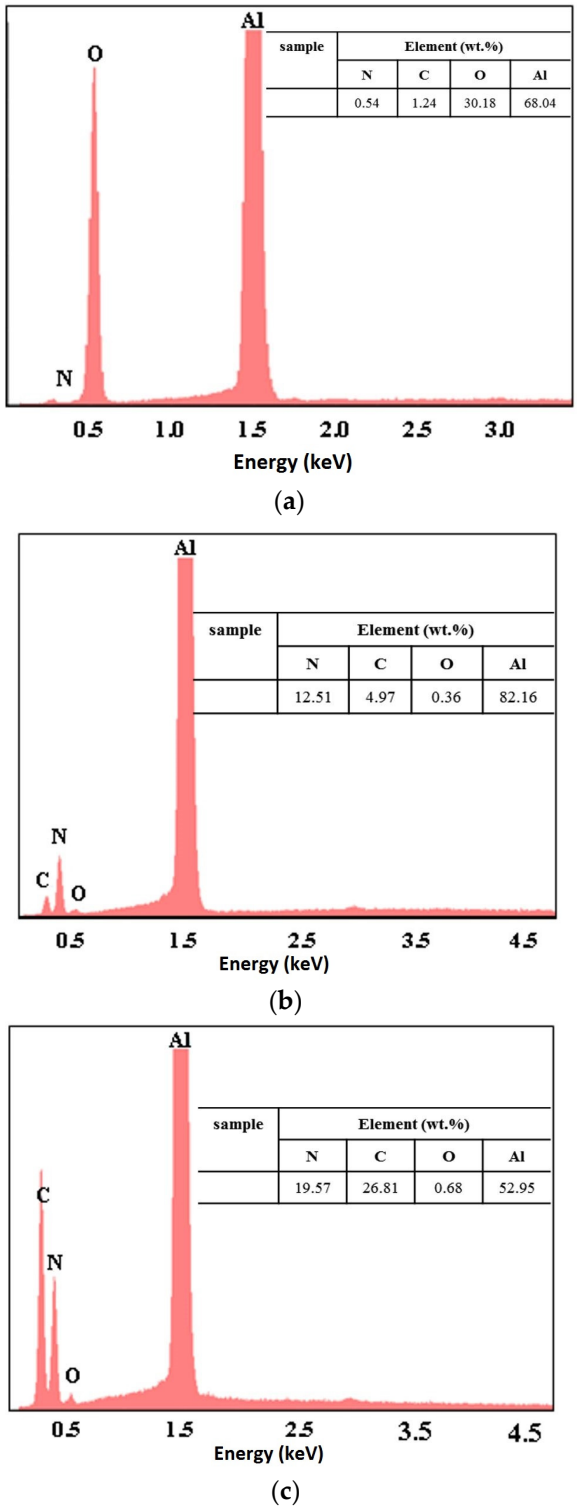

sample	Element (wt.%)			
	N	C	O	Al
	0.54	1.24	30.18	68.04

sample	Element (wt.%)			
	N	C	O	Al
	12.51	4.97	0.36	82.16

sample	Element (wt.%)			
	N	C	O	Al
	19.57	26.81	0.68	52.95

Figure 4. Energy X-ray dispersive spectroscopy (EDS) results of the AlN-coated carbon fibers obtained from AlCuF: (**a**) T15ANF; (**b**) T16ANF; (**c**) T17ANF.

The thermal conductivities of the composites were obtained by a hot disk method and the results of the experiment are exhibited in Figure 6. For ARCF reinforced polymer composites (ARCFP) without the AlN coating, the room-temperature thermal conductivity was 5.8 W/mK. With the addition of T15ANP, the value was similar to the thermal conductivity of ARCFP (5.6 W/mK) duo to the low

crystallinity of Al_2O_3-rich/AlN layer. However, with the addition of T17ANP, the thermal conductivity of the composites was significantly enhanced to 7.8 W/mK which is about 1.4 times larger than that of ARCFP without AlN. This result can be explained that the high content and crystallinity of AlN-rich layer on T17ANF possibly led to the high thermal conductivity of the T17ANP sample.

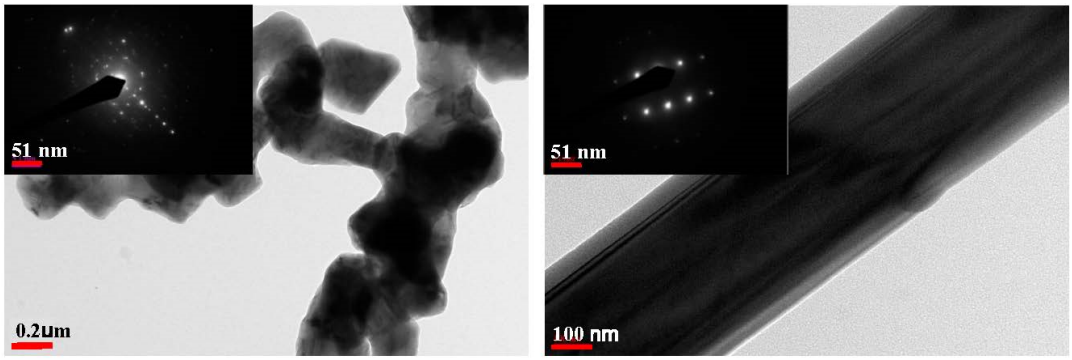

Figure 5. TEM images of coated materials on AlN layers with insert SEAD patterns: (**a**) T15ANF and (**b**) T17ANF.

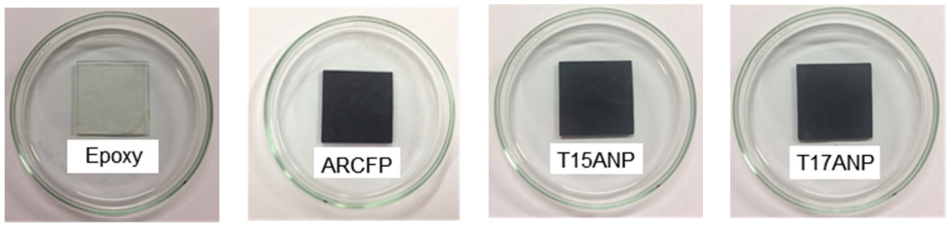

Figure 6. Thermal conductivity of carbon fibers-reinforced composites before and after AlN coating on fiber surfaces: (**a**) neat cured epoxy; (**b**) ARCF reinforced polymer composites (ARCFP); (**c**) T15ANP; and (**d**) T17ANP.

4. Conclusions

In this paper, AlN nanostructure has been synthesized on carbon fiber surfaces by the reactions between $AlCl_3$ and NH_3 gas via a direct wet-thermal method with a metallic catalyst under synthesis temperature of 1500 °C to 1700 °C. The effect of the copper coating on the AIN synthesis was confirmed by comparing the samples synthesized according to the presence or absence of the copper coating from the $AlCl_3$ treated carbon fibers. The elevated reaction temperature is beneficial for the growth of AlN, it was found that the temperature was a crucial experimental parameter in mediating the synthesis of AlN. The experimental results indicate that the obtained crystalline hexagonal AlN structure has high purity and consists of nanolayers. EDS and XRD profiles reveal that the yield of AlN nanostructures increased with the synthesis temperature up to 1700 °C in an ammonia (NH_3) gas atmosphere balanced by a nitrogen atmosphere. Higher temperature not only increases the density of AlN but also have good crystallinity, which together induces a fast synthesis rate by increasing surface diffusion. In addition, the synthesized AlN nanolayers could be applied as a reinforcement to produce polymers with high thermal conductivity.

Acknowledgments: This study was supported by a grant from the "National Research Foundation (NRF) of Korea (Project no. 2015M3A7B4049716)" funded by the Ministry of Science, Information & Communication Technology (ICT) and Future Planning (MSIP), Korea.

Author Contributions: Hyeon-Hye Kim is the main contributor to the article who performed the experiments. Analysis of the data was a joint effort by Youn-Sik Lee and Dong Chul Chung. Byung-Joo Kim conceived and designed the experiments as a corresponding author.

Conflicts of Interest: The authors declare no conflicts of interest.

References

1. Alok, A.; Alok, S. Development of a heat conduction model and investigation on thermal conductivity enhancement of AlN/epoxy composites. *Procedia Eng.* **2013**, *51*, 573–578.
2. Tomizawa, Y.; Sasaki, K.; Kuroda, A.; Takeda, R.; Kaito, Y. Experimental and numerical study on phase change material (PCM) for thermal management of mobile devices. *Appl. Therm. Eng.* **2016**, *98*, 320–329. [CrossRef]
3. Alshaer, W.G.; Nada, S.A.; Rady, M.A.; Barrio, E.P.D.; Sommier, A. Thermal management of electronic devices using carbon foam and PCM/nano-composite. *Int. J. Therm. Sci.* **2015**, *89*, 79–86. [CrossRef]
4. Wu, S.Y.; Huang, Y.L.; Ma, C.C.M.; Yuen, S.M.; Teng, C.C.; Yang, S.Y. Mechanical, thermal and electrical properties of aluminum nitride/polyetherimide composites. *Compos. Part A* **2011**, *42*, 1573–1583. [CrossRef]
5. Kim, J.H.; Kim, K.H.; Park, M.S.; Bae, T.S.; Lee, Y.S. Cu nanoparticle-embedded carbon foams with improved compressive strength and thermal conductivity. *Carbon Lett.* **2016**, *17*, 65–69. [CrossRef]
6. Bogner, M.; Hofer, A.; Benstetter, G.; Cruber, H.; Fu, R.Y.Q. Differential 3ω method for measuring thermal conductivity of AlN and Si_3N_4 thin films. *Thin Solid Films* **2015**, *591*, 267–270. [CrossRef]
7. Zhou, Y.; Hyuga, H.; Kusano, D.; Yoshizawa, Y.; Ohji, T.; Hirao, K. Development of high-thermal-conductivity silicon nitride ceramics. *J. Asian Ceram. Soc.* **2015**, *3*, 221–229. [CrossRef]
8. Kim, H.H.; Han, W.; Lee, H.S.; Min, B.G.; Kim, B.J. Preparation and characterization of silicon nitride coated carbon fibers and effects on thermal properties in composites. *Mater. Sci. Eng. B* **2015**, *200*, 132–138. [CrossRef]
9. Kim, K.J.; Kim, Y.W.; Lim, K.Y.; Nishimura, T.; Narimatsu, E. Electrical and thermal properties of SiC-AlN ceramics without sintering additives. *J. Eur. Ceram. Soc.* **2015**, *35*, 2715–2721. [CrossRef]
10. Chen, Y.C.; Lee, S.C.; Liu, T.H.; Chang, C.C. Thermal conductivity of boron nitride nanoribbons: Anisotropic effects and boundary scattering. *Int. J. Therm. Sci.* **2015**, *94*, 72–78. [CrossRef]
11. Kim, K.; Kim, J. Vertical filler alignment of boron nitride/epoxy composite for thermal conductivity enhancement via external magnetic field. *Int. J. Therm. Sci.* **2016**, *100*, 29–36. [CrossRef]
12. Yao, Y.; Zeng, X.; Guo, K.; Sun, R.; Xu, J.B. The effect of interfacial state on the thermal conductivity of functionalized Al_2O_3 filled glass fibers reinforced polymer composites. *Compos. Part A* **2015**, *69*, 49–55. [CrossRef]
13. Wang, S.; Zhang, D.; Ouyang, X.; Wang, Y.; Liu, G. Effect of one-dimensional materials on the thermal conductivity of Al_2O_3/glass composite. *J. Alloy. Compd.* **2016**, *667*, 23–28. [CrossRef]
14. Kim, B.J.; Bae, K.M.; An, K.H.; Park, S.J. Studies on the surface properties and thermal behaviors of modified Al_2O_3 nanofibers-reinforced epoxy composites. *Bull. Korean Chem. Soc.* **2012**, *33*, 3258–3264. [CrossRef]
15. Li, M.; Wan, Y.; Gao, Z.; Xiong, G.; Wang, X.; Wan, C.; Luo, H. Preparation and properties of polyamide 6 thermal conductive composites reinforced with fibers. *Mater. Des.* **2013**, *51*, 257–261. [CrossRef]
16. Zhou, S.; Chen, Y.; Zou, H.; Liang, M. Thermally conductive composites obtained by flake graphite filling immiscible polyamide 6/polycarbonate blends. *Thermochim. Acta* **2013**, *566*, 84–91. [CrossRef]
17. Rounaghi, S.A.; Eshghi, H.; Kiani Rashid, A.R.; Vahdati Khaki, J.; Samadi Khoshkhoo, S.; Scudino, S.; Eckert, J. Synthesis of nanostructured AlN by solid state reaction of Al and diaminomaleonitrile. *J. Solid State Chem.* **2013**, *198*, 542–547. [CrossRef]
18. Wang, Q.; Cui, W.; Ge, Y.; Chen, K.; Xie, Z. Carbothermal synthesis of spherical AlN granules: Effects of synthesis parameters and Y_2O_3 additive. *Ceram. Int.* **2015**, *41*, 6715–6721. [CrossRef]
19. Wu, H.M.; Peng, Y.W. Investigation of the growth and properties of single-crystalline aluminum nitride nanowires. *Ceram. Int.* **2015**, *41*, 4847–4851. [CrossRef]
20. Gao, Z.; Wan, Y.; Xiong, G.; Cuo, R.; Luo, H. Synthesis of aluminum nitride nanoparticles by a facile urea glass route and influence of urea/metal molar ratio. *Appl. Surf. Sci.* **2013**, *280*, 42–49. [CrossRef]
21. Chen, F.; Ji, X.; Zhang, Q. Enhanced field emission properties from AlN nanowires synthesized on conductive graphite substrate. *J. Alloy. Compd.* **2015**, *646*, 879–884. [CrossRef]

22. Radwan, M.; Bahgat, M.; El-Geassy, A.A. Formation of aluminum nitride whisker by direct nitridation. *J. Eur. Ceram. Soc.* **2006**, *26*, 2485–2488. [CrossRef]
23. Wang, H.; Yang, Q.; Jia, G.; Lei, R.; Wang, S.; Xu, S. Influence of yttrium dopant on the synthesis of ultrafine AlN powders by CRN route from a sol-gel low temperature combustion precursor. *Adv. Power Technol.* **2014**, *25*, 450–456. [CrossRef]
24. Shi, Z.; Radwan, M.; Kirihara, S.; Miyamoto, Y.; Jin, Z. Formation and evolution of quasi-aligned AlN nanowhiskers by combustion synthesis. *J. Alloy. Compd.* **2009**, *47*, 360–365. [CrossRef]
25. Xia, H.; Zhang, X.; Shi, Z.; Zhao, C.; Li, Y.; Wang, J.; Qiao, G. Mechanical and thermal properties of reduced graphene oxide reinforced aluminum nitride ceramic composites. *Mater. Sci. Eng. A* **2015**, *639*, 29–36. [CrossRef]
26. Aghdaie, A.; Haratizadeh, H.; Mousavi, S.H.; Jafari Mohammadi, S.A.; Oliveira, P.W. Effect of doping on structural and luminescence properties of AlN nanowires. *Ceram. Int.* **2015**, *41*, 2917–2922. [CrossRef]
27. Paul, R.K.; Lee, K.H.; Lee, B.T.; Song, H.Y. Formation of AlN nanowires using Al powder. *Mater. Chem. Phys.* **2008**, *112*, 562–565. [CrossRef]
28. Li, C. Strong cathodoluminescence of AlN nanowires synthesized by aluminum and nitrogen. *Mater. Lett.* **2014**, *115*, 212–214. [CrossRef]
29. Kim, H.W.; Kebede, M.A.; Kim, H.S. Temperature-controlled growth and photoluminescence of AlN nanowires. *Appl. Surf. Sci.* **2009**, *255*, 7221–7225. [CrossRef]
30. Chen, F.; Ji, X.; Zhang, Q. Radial AlN nanotips on carbon fibers as flexible electron emitters. *Carbon* **2015**, *81*, 124–131. [CrossRef]
31. Kim, D.K.; An, K.H.; Bang, Y.H.; Lee, K.K.; Oh, S.Y.; Kim, B.J. Effects of electrochemical oxidation of carbon fibers on interfacial shear strength using a micro-bond method. *Carbon Lett.* **2016**, *19*, 32–39. [CrossRef]
32. Raunija, T.S.K.; Supriya, N. Thermo-electrical properties of randomly oriented carbon/carbon composite. *Carbon Lett.* **2017**, *22*, 25–35.
33. Wonzniak, M.; Danelska, A.; Keta, D.; Szafran, M. New anhydrous aluminum nitride dispersions as potential heat-transferring media. *Powder Technol.* **2013**, *235*, 717–722. [CrossRef]
34. Wozniak, M.; Danelska, A.; Rultkowski, P.; Kata, D. Thermal conductivity of highly loaded aluminium nitride-poly(propylene glycol) dispersions. *Int. J. Heat Mass Transf.* **2013**, *65*, 592–598. [CrossRef]
35. Zyla, G.; Fal, J. Experimental studies on viscosity, thermal and electrical conductivity of aluminum nitride-ethylene glycol (AlN-EG) nanofludis. *Thermochim. Acta* **2016**, *637*, 11–16. [CrossRef]
36. Kim, S.; Song, Y.; Wright, J.; Heller, M.J. Graphene bi- and trilayers produced by a novel aqueous arc discharge process. *Carbon* **2016**, *102*, 339–345. [CrossRef]
37. Mashhadi, M.; Mearaji, F.; Tanizifar, M. The effects of NH_4Cl addition and particle size of Al powder in AlN whiskers synthesis by direct nitridation. *Int. J. Refract. Met. Hard Mater.* **2014**, *46*, 181–187. [CrossRef]
38. Radwan, M.; Bahgat, M. A modified direct nitridation method for formation of nano-AlN whiskers. *J. Mater. Process. Technol.* **2007**, *181*, 99–108. [CrossRef]
39. Niu, J.; Suzuki, S.; Yi, X.; Akiyama, T. Fabrication of AlN particles and whiskers via salt-assisted combustion synthesis. *Ceram. Int.* **2015**, *41*, 4438–4443. [CrossRef]
40. Qi, S.; Mao, X.; Li, X.; Feng, M.; Jiang, B.; Zhang, L. Synthesis of AlN hexagonal bipyramids by carbothermal reduction nitridation. *Mater. Lett.* **2016**, *174*, 167–170. [CrossRef]
41. Suehiro, T.; Tatami, J.; Meguro, T.; Matsuo, S.; Komeya, K. Morphology-retaining synthesis of AlN particles by gas reduction-nitridation. *Mater. Lett.* **2002**, *57*, 910–913. [CrossRef]
42. Liu, G.; Dai, P.; Wang, Y.; Yang, J.; Qiao, G. Fabrication of pure SiC ceramic foams using SiO_2 as a foaming agent via high-temperature recrystallization. *Mater. Sci. Eng. A* **2011**, *528*, 2418–2422. [CrossRef]
43. Wastson, I.M. Metal organic vapour phase epitaxy of AlN, GaN, InN and their alloys: A key chemical technology for advanced device application. *J. Coord. Chem.* **2013**, *257*, 2120–2141. [CrossRef]
44. Bakina, O.V.; Svarovskaya, N.V.; Glazkova, E.A.; Lozhkomoev, A.S.; Khorobraya, E.G.; Lerner, M.I. Flower-shaped ALOOH nanostructures synthesized by the reaction of an AlN/Al composite nanopowder in water. *Adv. Powder Technol.* **2015**, *26*, 1512–1519. [CrossRef]
45. Lei, M.; Song, B.; Guo, X.; Guo, Y.F.; Li, P.G.; Tang, W.H. Large-scale AlN nanowires synthesized by direct sublimation method. *J. Eur. Ceram. Soc.* **2009**, *29*, 195–200. [CrossRef]
46. Wu, H.; Qin, M.; Chu, A.; Wan, Q.; Cao, Z.; Liu, Y.; Qu, X.; Volinsky, A.A. AlN powder synthesis by sodium fluoride-assisted carbothermal combustion. *Ceram. Int.* **2014**, *40*, 14447–14452. [CrossRef]

47. Peebles, L.H. *Carbon Fibers: Formation, Structure and Properties*; CRC Press: Boca Raton, FL, USA, 1995.
48. Keyan, Z.; Lianshan, W.; Jin, C.S.; Thompson, C.V. Structural analysis of metalorganic chemical vapor deposited AlN nucleation layers on Si (111). *J. Cryst. Growth* **2004**, *268*, 515–520.
49. Kukushkin, S.A.; Osipov, A.V.; Bessolov, V.N.; Medvedev, B.K.; Nevolin, V.K.; Tcarik, K.A. Substrates for epitaxy of gallium nitride: New materials and techniques. *Rev. Mater. Sci.* **2008**, *17*, 1–32.
50. Mohammed Sadiq, I.; Pakrashi, S.; Chandrasekaran, N.; Mukherjee, A. Studies on toxicity of aluminum oxide (Al_2O_3) nanoparticles to microalgae species: *Scenedesmus* sp. and *Chlorella* sp. *J. Nanopart. Res.* **2011**, *13*, 3287–3299. [CrossRef]
51. Kong, S.; Wei, H.; Yang, S.; Li, H.; Feng, Y.; Chen, Z.; Liu, X.; Wang, L.; Wang, Z. Morphology and structure controlled growth of one-dimensional AlN nanorod arrays by hydride vapor phase epitaxy. *RSC Adv.* **2014**, *4*, 54902–54906. [CrossRef]
52. Shen, L.; Cheng, T.; Wu, L.; Li, X.; Cui, Q. Synthesis and optical properties of aluminum nitride nanowires prepared by arc discharge method. *J. Alloy. Compd.* **2008**, *465*, 562–566. [CrossRef]